frontiers | Frontiers in Ecology and Evolution

ORIGINAL RESEARCH
published: 06 April 2022
doi: 10.3389/fevo.2022.843714

Changes in Landscape Pattern and an Ecological Risk Assessment of the Changshagongma Wetland Nature Reserve

Cai Yang[1], *Wei Deng*[1,2]*, *Quanzhi Yuan*[1,2] *and Shaoyao Zhang*[1,2]

[1] School of Geography and Resource Science, Sichuan Normal University, Chengdu, China, [2] Research Center for Resource, Environment and Sustainable Development in West Sichuan, Chengdu, China

The Changshagongma wetlands is the Chinese National Nature Reserve were listed as a Ramsar Wetland of International Importance in 2018. Here, we examined four periods (1992, 2002, 2013, and 2020) of remote sensing image data to analyze the changes in wetland landscape patterns and the ecological risk in Changshagongma Wetland Nature Reserve over the past 30 years. The results showed that wetlands account for approximately 30% of the study area, and swamp meadows were the main type of wetland, accounting for approximately 95% of the total wetland area. In terms of landscape patterns, wetland fragmentation declined, wetland patch shapes became less complicated, and spatial connectivity increased. The landscape fragmentation of non-wetland alpine meadows was reduced. The patches of sandy grasslands tended to be regular, and their spatial connectivity was reduced. The wetland regions of high ecological risk are concentrated in the central and southern parts of the Changshagongma Wetland Nature Reserve. Low-risk regions are mainly concentrated in the contiguous swamp meadows in the northwest and wetlands in the southwest. From 1992 to 2020, the level of ecological risk of the Changshagongma Wetland Nature Reserve showed a "∧"-shaped trend, with the highest risk in 2002 and the lowest risk in 2020. Among the selected indicators, climate conditions constituted the main factor affecting the ecological risk of the Changshagongma Wetland Nature Reserve, followed by topographical conditions, and human activities were the least influential. Over the past 30 years, the temperature and precipitation in the study area increased significantly. The climate in the study area can be roughly divided into two periods bounding 2002, and the climate has been changing from cold and dry to warm and wet. The ecological environment of the study area is affected by natural and human activities. Cold and dry climatic conditions and uncontrolled grazing accelerate the destruction of the wetland ecological environment, and warm and wet climatic conditions and ecological conservation policies are conducive to the ecological restoration of wetlands. In general, the wetland landscape structure in the study area has become less complex, landscape heterogeneity has decreased, and ecological quality has improved.

Keywords: Changshagongma wetlands, wetland landscape, pattern change, geodetector, landscape ecological risk

OPEN ACCESS

Edited by:
Mauro Fois,
University of Cagliari, Italy

Reviewed by:
Jakub Nowosad,
Adam Mickiewicz University, Poland
Junhong Bai,
Beijing Normal University, China
Zhenguo Niu,
Aerospace Information Research Institute (CAS), China

***Correspondence:**
Wei Deng
dengwei@sicnu.edu.cn

Specialty section:
This article was submitted to Environmental Informatics and Remote Sensing, a section of the journal Frontiers in Ecology and Evolution

Received: *26 December 2021*
Accepted: *28 February 2022*
Published: *06 April 2022*

Citation:
Yang C, Deng W, Yuan Q and Zhang S (2022) Changes in Landscape Pattern and an Ecological Risk Assessment of the Changshagongma Wetland Nature Reserve. Front. Ecol. Evol. 10:843714. doi: 10.3389/fevo.2022.843714

INTRODUCTION

Landscape patterns refer to the spatial arrangement and combination of landscape patches of different shapes and sizes. Different landscape patterns are formed under the combined effects of various ecological processes. Since the 1980s, landscape ecology methods have been gradually applied to wetland research. With these applications, the analysis of changes in landscape patterns has become a focus of wetland ecology research (Cong et al., 2019; Shen et al., 2019). Changes in wetland landscape patterns refer to changes in landscape distribution and composition caused by conversion between landscape classes. Changes in wetland landscape patterns can be divided into three categories: conversion from wetland to non-wetland, conversion from non-wetland to wetland, and conversion between different subclasses of wetland. Landscape class changes have two types of causes: human activities and natural factors (Bai et al., 2013; Liu et al., 2014). Remote sensing technology has been widely used in wetland research (Huang et al., 2018; Mahdavi et al., 2018; Wang et al., 2021). In recent years, cutting-edge technologies such as big data and cloud computing have been developing rapidly. Google Earth Engine (GEE) is a cloud-based platform, that combines a multi-petabyte catalog of satellite imagery and geospatial datasets with planetary-scale analysis capabilities. Its advantages include rich data, excellent performance, diverse algorithms, and an open system (Kumar and Mutanga, 2018). It is an important tool for image classification and is widely used in the study of wetland changes (Wang et al., 2020; Chen and Zhu, 2021; Cui et al., 2021; Yao et al., 2021).

Regional landscape ecological risk assessment is an important foundation for regional conservation, and it plays an important role in elucidating the distribution and trends of regional ecological risks and implementing targeted ecological conservation (Santos et al., 2006; Liu et al., 2008). The essence of change in landscape patterns is characterized long-term cumulative changes in the use mode and use intensity of landscape classes. Researchers have conducted a great amount of research on ecological risk assessment based on landscape pattern metrics. Using landscape patterns to construct a landscape ecological risk model has become an important method of ecological risk assessment (Shi et al., 2015; Jin et al., 2019). Exploring the factors driving regional ecological risks provides active guidance for improving the regional conservation approach. As an important tool for detecting driving factors that cause spatial heterogeneity, Geodetector has been widely used in many research fields by researchers and has generated excellent application results (Du et al., 2017; Wang et al., 2019; Yuan et al., 2019; Chen et al., 2020; Zhu et al., 2020).

The Qinghai-Tibet Plateau is rich in alpine wetland resources, and its wetlands account for approximately 20% of China's total wetland area. It is one of the most important regions for wetland functions in China (Zhao et al., 2015). Located on the eastern portion of the Qinghai-Tibet Plateau, the Changshagongma Wetland Nature Reserve is an alpine wetland region. It is also an important component of the source region of the Yangtze River and the Yellow River. The region is characterized by harsh climatic conditions and a fragile natural environment. It is considered uninhabitable, and nomadism is the main way of life for humans in the region. Relatively few studies have been conducted on these wetlands because of their remote location, and research on landscape patterns and ecological risks of wetlands under the influence of climate change is especially lacking.

Choosing an appropriate spatial scale and conducting a landscape ecological risk assessment based on the ecological significance of landscape pattern metrics hold practical significance for wetland landscape ecological research (Jin et al., 2019; Hou et al., 2020). The specific steps taken in this study were as follows: (1) Based on the GEE platform, four periods of data (1992, 2002, 2013, and 2020) on the Changshagongma wetlands were extracted, and landscape pattern metrics were selected at the class level and landscape level to analyze the changes in landscape pattern. (2) Landscape pattern metrics were used to construct a landscape ecological risk model, and the ecological risk of the wetlands in the study area was assessed. (3) Factors driving the wetlands' ecological risk were analyzed using Geodetector.

MATERIALS AND METHODS

Study Area

The Changshagongma Wetland Nature Reserve is on the eastern portion of the Qinghai-Tibet Plateau, located at 97°22′–98°39′ E and 33°18′-34°12′ N (average elevation of 3,840–5,249 m), adjacent to Sanjiangyuan National Park in Qinghai Province, within the boundary of Shiqu County, Ganzi Tibetan Autonomous Prefecture, Sichuan Province (**Figure 1**). Its total area is approximately 6,700 km^2. The dimensions are 100 km from north to south and approximately 120 km from east to west. The climate is cold, with short spring and autumn seasons, rainy summers, and severely cold and dry winters. The annual average temperature is –2 to 0.7°C, and the annual precipitation is 360–820 mm. Topographically, the reserve is a typical hilly plateau. The Zhaqu River basin in the north belongs to the Yellow River basin, and the remaining rivers are in the Yangtze River basin. Many wetlands are within the reserve's boundaries, including swamp meadows, lake wetlands, and riverine wetlands. It is an important water conservation area in the upper reaches of the Yangtze River and the Yellow River and holds high research and conservation value.

Data

The data used in this study included remote sensing imagery, digital elevation model (DEM) data, aspects, slopes, relief amplitude, temperatures, evapotranspiration, precipitation, protected area boundaries, and roads. The remote sensing data were obtained from Landsat images (**Table 1**) provided by the GEE platform.[1] To improve the quality of the extracted wetland data as much as possible, the time periods were limited to June to September, and images with a cloud cover of less than 15% were selected as available images, and the

[1]https://developers.google.cn/earth-engine/datasets/catalog/landsat

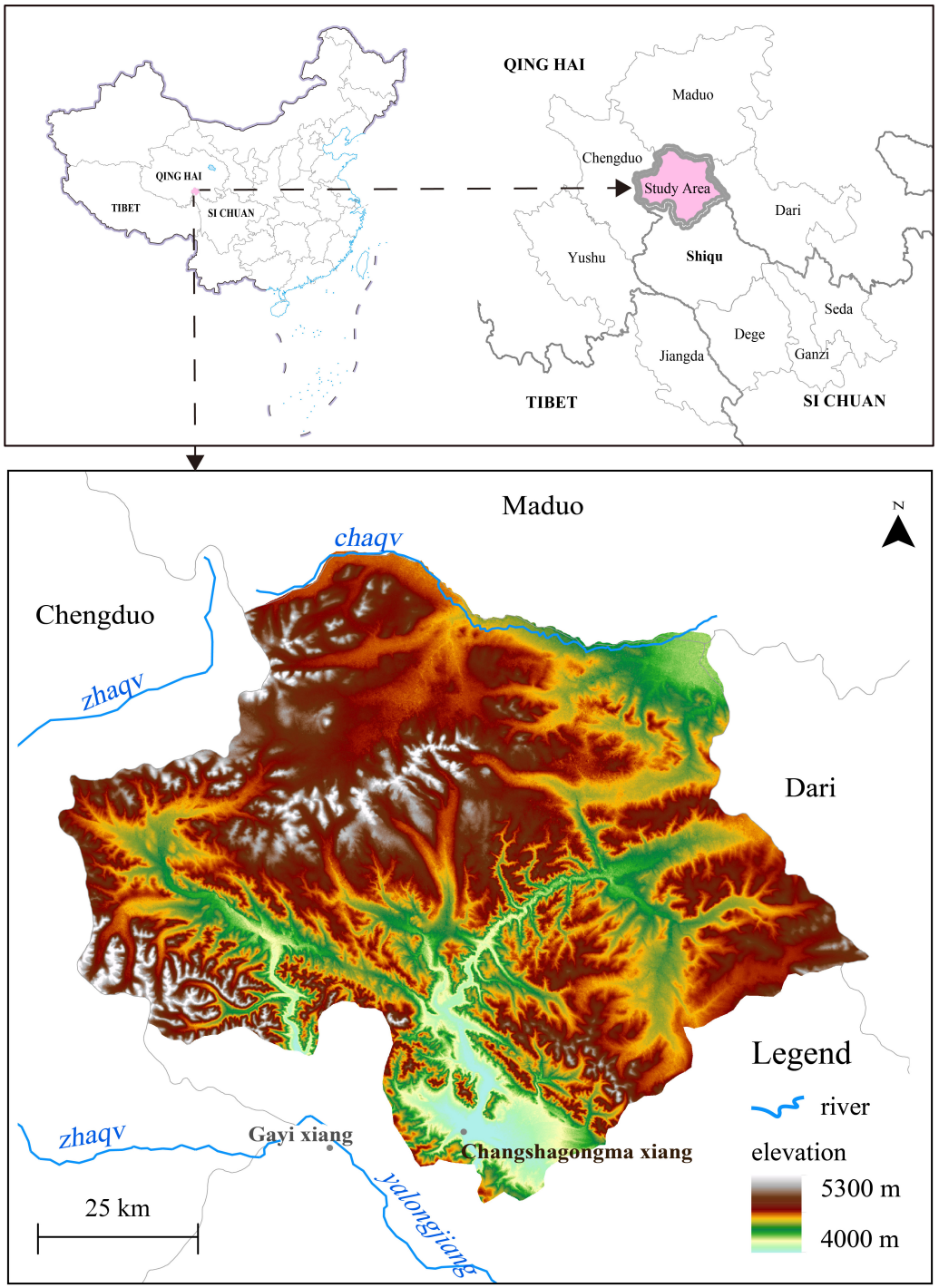

FIGURE 1 | Geographical location of the Changshagongma Wetland Nature Reserve.

appropriate image was chosen from them as the base image. Then, according to the cloud coverage area of the basic image data, the available image data of the adjacent time period are selected as the supplementary image data of the cloud coverage area. Cloud removal, geometric correction, fusion splicing, and image cropping were conducted on the GEE cloud platform to obtain four periods of image data (1992, 2002, 2013, and 2020). The meteorological station measurement data were obtained from the China Meteorological Data Service Center,[2] and meteorological station measurement data were used for climate

[2]http://data.cma.cn

TABLE 1 | Landsat images used in this study.

	Base images		Supplementary images			
	Date	Tract number	Date	Tract number	Date	Tract number
1992	03.08.1992	134036	16.06.1992	134036		
	03.08.1992	134037	16.06.1992	134037		
2002	15.08.2002	134036	17.07.2003	134036		
	15.08.2002	134037	17.07.2003	134037		
2013	13.08.2013	134036	16.08.2014	134036		
	13.08.2013	134037	16.08.2014	134037		
2020	17.09.2020	134036	25.08.2020	134037	02.07.2021	134036
	17.09.2020	134037	29.06.2020	134036	02.07.2021	134037
			29.06.2020	134037		

trend analysis. The gridded meteorological data were obtained from the National Earth System Science Data Center of the National Science and Technology Infrastructure,[3] with a spatial resolution of 1 km, and were resampled in spatial resolution (3 km) for driving force analysis. The DEM data were from the Geospatial Cloud,[4] with a resolution of 30 m and were resampled in spatial resolution (3 km) for driving force analysis. Slope, aspect, and relief amplitude were calculated using the DEM data. The boundaries of the study area were obtained from the Chinese Nature Reserve Specimen Resource Sharing Platform.[5] Road data were derived through vectorization from Google Earth historical images. The data used the same projection coordinate system (UTM Zone 47N).

Spatiotemporal changes in regional ecological risks result from the combined effects of multiple factors. This paper selected eight indicators, including topography and geomorphology (aspect X_1, elevation X_2, slope X_3, and relief amplitude X_4), climatic characteristics (annual evapotranspiration X_5, annual precipitation X_6, and annual average temperature X_7), and human disturbance (distance from road X_8). The driving force was detected by using the geographic detector model. Since the dependent variables in Geodetector must be categorical variables, X_1 was divided into eight categories based on the situation in the study area. X_2, X_3, X_4, and X_8 were each divided into five categories using the natural breaks method. The remaining climatic variables were divided into seven categories each.

Methodology

Extraction of Wetland Information

The landscape in the study area was classified into wetlands and non-wetlands based on the existing relevant classification standards in combination with field investigations. The wetland landscape included three subclasses: swamp meadows, lake wetlands, and riverine wetlands. Non-wetlands included three subclasses: alpine meadows, sandy grasslands, and alpine bare rocks. By referring to previous experiences and practical conditions, the interpretation signs of subclasses were established (**Table 2**). We used the support vector machine (SVM) classifier within the Google Earth Engine (GEE) cloud-computing platform to classify the images and manual visual interpretation and correction based on field survey data and Google Earth historical images. Finally, the accuracy of the classification was evaluated by calculating the overall classification accuracy and Kappa coefficient through the confusion matrix.

Landscape Pattern Metrics Selection

Landscape pattern metric analysis is a common method for studying the history of wetland landscape patterns. Landscape pattern metrics can greatly condense landscape spatial pattern information and reflect its structural and spatial configuration. Metrics for landscape patterns are usually computed and analyzed at the patch level, class level, and landscape level (Bai et al., 2013). The selection of appropriate landscape metrics is useful for understanding regional landscape patterns (Inkoom et al., 2018; Ma et al., 2019). This article analyzed the changes in the landscape pattern metrics from two perspectives: the class level and the landscape level. The selected class-level metrics included the percentage of landscape (PLAND), patch density (PD), aggregation index (AI), and mean fractal dimension (FRAC_MN). The selected landscape-level metrics included edge density (ED), PD, contagion index (CONTAG), and the Shannon's diversity index (SHDI). See the related literature for specific concepts, calculation methods, and the ecological significance of the metrics (Li and Wu, 2004; Wu, 2004). The calculation of these metrics was completed using the Fragstats 4.2.1 software package. At the same time, a bivariate correlation analysis was carried out between the landscape pattern index and the eight selected indicators ($X_1 - X_8$).

Landscape Ecological Risk Assessment

Based on the concept and connotation of landscape ecological risk (Shi et al., 2015; Jin et al., 2019; Yue et al., 2021), a landscape ecological risk index (*LERI*) can be constructed using a landscape disturbance ecological index (*E*) and fragile index (*F*) (Pei et al., 2014). To characterize the spatial distribution of ecological risks, the study area was divided into 739 ecological risk cells with a grid of 3 km × 3 km according to equal distance sampling methods. 3 km × 3 km The calculation formula of the landscape ecological risk index ($LERI_k$) for each assessment cell is as follows:

$$LERI_k = \sum_{i=1}^{n} \frac{A_i}{A} (E_i \times F_i)$$

where $LERI_k$ is the landscape ecological risk index value for the k^{th} cell evaluated. A_i is the area of land cover type i in the k^{th} risk assessment cell. A is the area of the k^{th} risk assessment cell. E_i is the landscape disturbance ecological index value for land cover class *i*. F_i is the landscape fragility index value of land cover class *i*. The value for the landscape vulnerability fragile index can be determined using an expert scoring method.

The landscape disturbance ecological index (E_i) characterizes the extent to which a landscape is affected by natural or human activities. It can be expressed using the area-weighted mean shape index, fractal dimension, and landscape dominance. The formula

[3]http://www.geodata.cn

[4]http://www.gscloud.cn/

[5]http://www.papc.cn/

TABLE 2 | Image example of landscape type.

Major Type	Wetlands			Non-wetlands		
Minor Type	**Swamp meadows**	**Lake wetlands**	**Riverine wetlands**	**Alpine meadows**	**Sandy grasslands**	**Alpine bare rocks**
Image example						

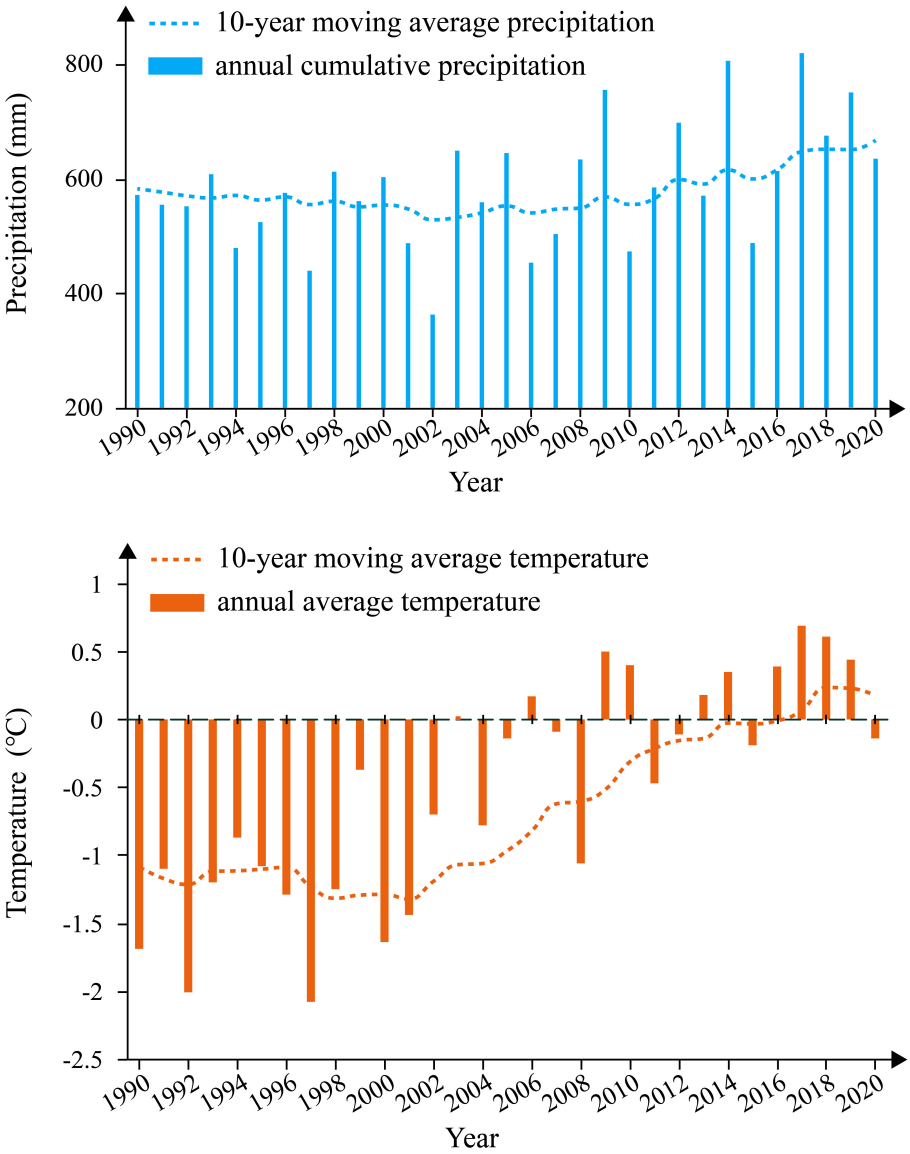

FIGURE 2 | Trends of temperature and precipitation at the Shiqu County Weather Station from 1990 to 2020.

is

$$E_i = (\alpha \times AWMSI_i + \beta \times FD_i + \gamma \times S_i) \times D_i$$

where $AWMSI_i$ is the area-weighted mean shape index, which is an important indicator for measuring the complexity of a landscape's spatial pattern; generally, the more complex the landscape is, the stronger the disturbance of the assessment unit by the natural environment or human activities. FD_i is the fractal dimension, which reflects the shape complexity of patches and landscape patterns at a certain observational scale and can represent the impacts of human activities or the natural environment on the landscape pattern. S_i is the landscape dispersion index, which reflects the fragmentation degree of landscape patches on a certain spatial scale and can represent

TABLE 3 | Image classification accuracy verification.

	1992	2002	2013	2020
Overall accuracy (%)	88.0	87.3	85.7	86.7
Kappa coefficient	0.855	0.845	0.825	0.838

the degree of influence of the natural environment or human activities on the landscape pattern. D_i is the landscape dominance index, which reflects the dominant landscape in the evaluation unit, and the dominant landscape plays a leading role in the changing process of the landscape pattern. α, β, and γ are the weights of the three corresponding metrics, and $\alpha + \beta + \gamma = 1$. Referring to the existing research results and considering the situation in the study area, the values of 0.5, 0.3, and 0.2 were assigned to α, β, and γ, respectively. The indicators were normalized during the calculation.

Landscape fragility (F_i) characterizes the vulnerability of different land use classes. The higher its value is, the higher the ecological risk. Based on the existing research and the situation in the study area, an expert scoring method can be used to determine the vulnerability of a landscape class. From high vulnerability to low vulnerability, the classes were ranked as sandy grasslands 7, alpine meadows 6, riverine wetlands 5, lake wetlands 4, swamp meadows 3, and alpine bare rocks 1. The weights were normalized before calculation.

The Geodetector Model

Geodetector is a spatial analysis method developed and continuously improved by Wang et al. This method is mainly used in research on the mechanisms of spatial differentiation. The core concept is based on the assumption that if an independent variable has an important influence on a dependent variable, then the spatial distribution of the independent variable should resemble the spatial distribution of the dependent variables (Wang and Xu, 2017). The model includes four components: the factor detector, interaction detector, risk detector, and ecological detector. This article used the factor detector to reveal the driving factors that influence the spatial differentiation of ecological risks in the study area. The factor detector is used to detect whether a certain geographical factor causes of the spatial differentiation of a certain geographical feature and its power of explanation (q). The formula for the factor detector is

$$q = 1 - \frac{\sum_{h=1}^{L} N_h \sigma_h^2}{N\sigma^2}$$

where N and σ^2 represent the number of the independent variable's partition cells and the variance in the dependent variable Y in the region, respectively. L is the number of strata of the independent variable ($h = 1, 2, \cdots, L$), N_h and σ_h^2 are the number of partition cells and variance in the independent variable, respectively, corresponding to dependent variable Y at stratum h.

RESULTS

Climate Change Trend Analysis

Based on the annual cumulative precipitation (PRE) and annual average temperature (TMP) data from the Shiqu County Weather Station, the 10-year moving average precipitation (PRE-AVG) and 10-year moving average temperature (TMP-AVG) were calculated and used as references to analyze climate trends in the study area. As shown in **Figure 2**, based on the changes in the 10-year moving annual average precipitation and annual average temperature, precipitation and temperature showed gradual, fluctuating declines before 2002. After 2002, clear but fluctuating increases occurred. Additionally, the degree of decline in the early period (1992–2002) was smaller than the degree of increase in the later period (2002–2020). Over the past 30 years, temperature and precipitation in the study area have increased, and the increase in temperature has been more obvious than that in precipitation. In terms of the climatic characteristics of the selected time periods, the annual precipitation was 555.8 mm in 1992, 366.9 mm in 2002, 574.2 mm in 2013, and 638.8 mm in 2020. The precipitation in 2002 was significantly lower than the 10-year average of 529.2 mm and much lower than the 30-year average of 589.8 mm. The annual average temperature was −2.01°C in 1992, −0.70°C in 2002, 0.18°C in 2013, and 0.14°C in 2020. The average temperature in 2002 was significantly higher than the 10-year moving average temperature of −1.19°C. The average annual temperature exceeded 0°C in 2003, and the 10-year moving annual average temperature has been higher than 0°C since 2017, indicating a further increase in temperature. Overall, the climate in the study area changed from cold and dry to warm and wet.

Changes in Landscape Distribution and Area

The accuracy of the classification was evaluated, and the overall accuracy of the classification results for all four periods was found to exceed 85% (**Table 3**). Therefore, the classification results of the four periods (**Figure 3**) met the research requirements.

As seen in **Figure 3**, swamp meadows and alpine meadows were the main landscape classes. Swamp meadows were mainly located in the north and southeast. Riverine wetlands were widely distributed in valleys between hills. Lake wetlands were mainly found in the north. Alpine meadows were mostly distributed in the central and southern regions. Sandy grasslands were mainly located in the central and western regions. Alpine bare rocks were mainly distributed in the alpine snow-covered areas in the western, southwestern, and central regions. As seen in **Table 4**, among the wetland subclasses in the study area, swamp meadows was the main type of wetlands with the largest area, followed by riverine wetlands, and then lake wetlands. Overall, the wetland area in the study area first decreased and then increased. Among the subclasses, swamp meadows decreased from 1909.83 km^2 (28.46%) in 1992 to 1748.96 km^2 (26.07%) in 2002, then increased to 1892.16 km^2 (28.20%) in 2013 and increased to 1943.79 km^2 (28.97%) in 2020. Riverine wetlands decreased from 80.99 km^2 (1.21%) in 1992 to 70.87 km^2 (1.06%) in 2002, then increased to

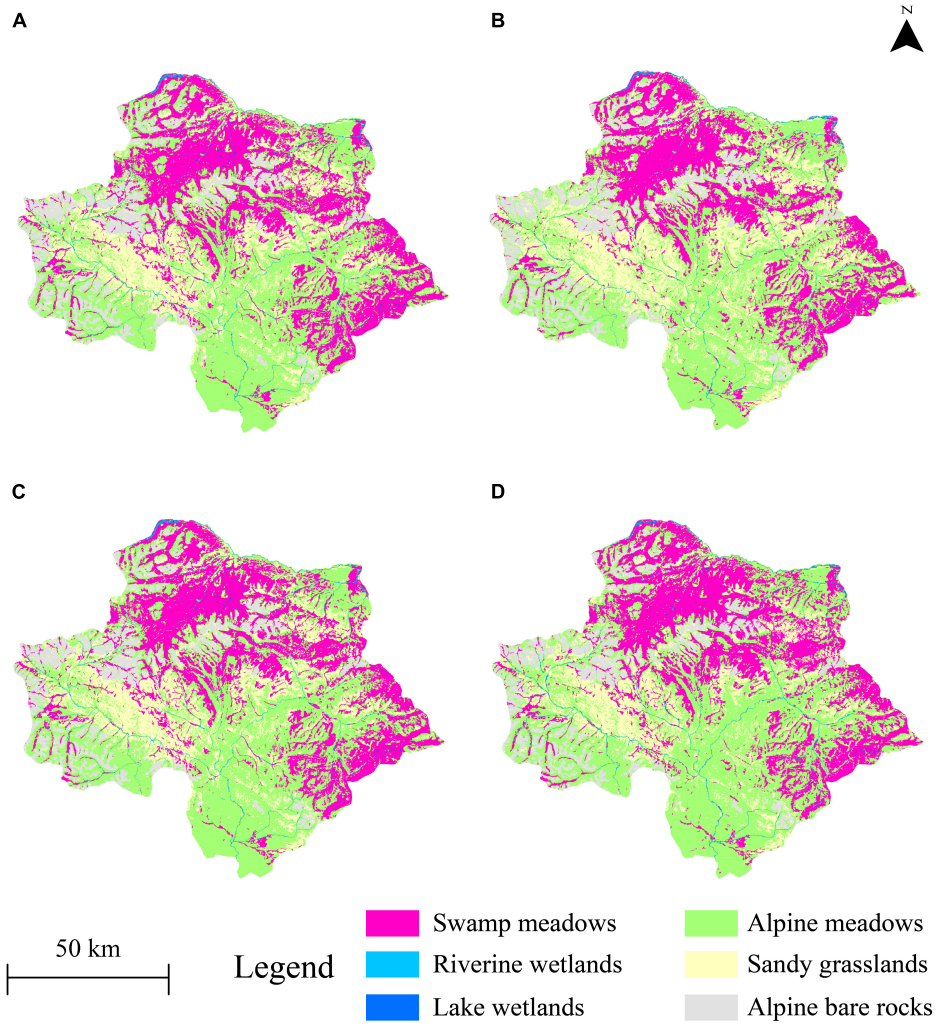

FIGURE 3 | Distribution of various landscape types in the Changshagongma Wetland Nature Reserve in the four periods. **(A)** 1992, **(B)** 2002, **(C)** 2013, **(D)** 2020.

80.79 km^2 (1.20%) in 2013 and increased slightly to 81.55 km^2 (1.22%) in 2020. Lake wetlands decreased from 9.70 km^2 (0.14%) in 1992 to 7.49 km^2 (0.11%) in 2002, then increased to 9.35 km^2 (0.14%) in 2013 and decreased slightly to 9.22 km^2 in 2020. The change in the area of alpine meadows was the same as that of wetland area. It decreased from 2926.90 km^2 (43.62%) in 1992 to 2889.74 km^2 (43.07%) in 2002, and then increased to 2983.60 km^2 (44.47%) in 2013 and to 3133.04 km^2 (46.69%) in 2020. The change in the area of sandy grasslands was opposite to the change in wetland area. The area of this subclass increased from 1204.18 km^2 (17.95%) in 1992 to 1416.28 km^2 (21.11%) in 2002, then declined to 1169.00 km^2 (17.42%) in 2013 and decreased to 966.15 km^2 (14.4%) in 2020. Alpine bare rocks were relatively stable with small changes in area. The total area of this subclass was approximately 576 km^2 (8.59%). Comparing the climatic trends among the time periods, the precipitation decreased from 1992 to 2002, and the wetland area was smallest in 2002, when the annual precipitation was the lowest. The precipitation increased significantly from 2002 to 2020, and the wetland area also increased significantly after 2002, indicating that precipitation affected the change in wetland area.

Landscape Pattern Metrics Analysis

Metric Changes at the Class Level

The landscape pattern metrics at the class level for the Changshagongma Wetland Nature Reserve in the four periods were calculated (**Figure 4**). PLAND is the percentage of a type of landscape in the total area, and the largest area is the main landscape, which is the dominant landscape in the study area. As shown in **Figure 4A**, the PLAND values over the four periods were ranked in descending order as alpine meadows > swamp meadows > sandy grasslands > alpine bare rocks > riverine wetlands > lake wetlands. The PLAND values of alpine meadows, swamp meadows, and sandy grasslands were significantly higher than those of other landscape classes. Alpine meadows were always the largest and dominant landscape in the study area. In comparison, the PLAND values of swamp meadows, alpine meadows, and sandy grasslands showed obvious fluctuations,

TABLE 4 | Area (km^2) and percentage (%) of various landscape classes at the Changshagongma Wetland Nature Reserve during the four time periods.

Landscape type		1992		2002		2013		2020	
Major type	**Minor type**	**Area**	**%**	**Area**	**%**	**Area**	**%**	**Area**	**%**
Wetlands	1	1909.83	28.46	1748.96	26.07	1892.16	28.20	1943.79	28.97
	2	80.99	1.21	70.87	1.06	80.79	1.20	81.55	1.22
	3	9.70	0.14	7.49	0.11	9.35	0.14	9.22	0.14
Non-wetlands	4	2926.90	43.62	2889.74	43.07	2983.60	44.47	3133.04	46.69
	5	1204.18	17.95	1416.28	21.11	1169.00	17.42	966.15	14.40
	6	578.32	8.62	576.57	8.59	575.02	8.57	576.05	8.59
Total		6709.92	100.00	6709.91	100.00	6709.92	100.00	6709.80	100.00

1, swamp meadows; 2, riverine wetlands; 3, lake wetlands; 4, alpine meadows; 5, sandy grasslands; and 6, alpine bare rocks.

while those of riverine wetlands, lake wetlands, and alpine bare rocks displayed smaller fluctuations. The trends in PLAND values were similar for alpine and swamp meadows, first decreasing and then increasing. The minimum values occurred in 2002 (43.07% for alpine meadows and 26.07% for swamp meadows), and the maximum values occurred in 2020 (46.69% for alpine meadows and 28.95% for swamp meadows). In comparison, the PLAND values of sandy grasslands first increased and then decreased. The maximum value appeared in 2002 at 21.11%, and the minimum value appeared in 2020 at 14.40%. The PLAND values of riverine wetlands, lake wetlands, and alpine bare rocks fluctuated slightly. These results show that over the past 30 years, the changes in swamp meadows, alpine meadows, and sandy grasslands dominated the main process of landscape pattern change.

PD can reflect the level of fragmentation of a landscape class. The larger its value is, the more fragmented the landscape class, and vice versa. **Figure 4B** indicates that the levels of fragmentation were the highest for sandy grasslands and alpine meadows and were lower for wetlands (swamp meadows, riverine wetlands, and lake wetlands) and alpine bare rocks. The level of sandy grasslands fragmentation changed significantly from 1992 to 2020. The PD of sandy grasslands increased from 1.29 in 1992 to 1.59 in 2002, increased to a maximum value of 1.80 in 2013, and then decreased to a minimum value of 1.27 in 2020. The PD values of alpine meadows first decreased from 1.30 in 1992 to 1.14 in 2002, then increased to the highest value of 1.78 in 2013, and then decreased to the lowest value of 1.07 in 2020. The PD values of swamp meadows decreased from 0.22 in 1992 to the lowest value of 0.18 in 2002 and remained unchanged after increasing to 0.21 in 2013. The PD values of the other classes did not change significantly. Overall, landscape fragmentation at the class level decreased from 1992 to 2020.

AI can reflect the degree of aggregation and disaggregation of a landscape class. The greater its value is, the higher the degree of landscape aggregation. The lower its value is, the less aggregated the landscape. As shown in **Figure 4C**, the aggregation levels of the landscape classes in the study area were ranked from high to low as swamp meadows > alpine bare rocks > alpine meadows > sandy grasslands > riverine wetlands > lake wetlands. All AI values for swamp meadows in the four periods exceeded 95, indicating that the spatial connectivity of swamp meadows was very high. The AI values of alpine bare rocks and alpine meadows were greater than 90, indicating their high spatial connectivity. The AI values of riverine wetlands and lake wetlands was lower, indicating that riverine wetlands and lake wetlands were relatively disaggregated. The AI values of wetlands increased from 1992 to 2020, indicating that the spatial connectivity of wetlands increased. Among the non-wetlands, the AI values of sandy grasslands tended to decrease, and the area of sandy grasslands decreased, indicating that the connectivity of sandy grasslands decreased, and sandy of sandy grasslands became spatially smaller and more isolated.

FRAC_MN can reflect the shape of a patch. The higher its value is, the greater the shape deviates from a square and the more irregular the distribution, and vice versa. **Figure 4D** shows that the FRAC_MN values of various landscape classes were ranked from high to low as riverine wetlands > alpine bare rocks > swamp meadows > alpine meadows > sandy grasslands > lake wetlands. The FRAC_MN values for riverine wetlands was significantly higher than those of other landscape classes because rivers are linearly distributed and their shapes are extremely irregular. The FRAC_MN values for lake wetlands was significantly lower than those of other landscape classes because the lake wetlands are mostly clusters with regular shapes. The FRAC_MN values for swamp meadows was relatively high because their area is greatly affected by the topography of the study area; most swamp meadows are in strips with irregular shapes. Alpine bare rocks are distributed along the belt-shaped mountain ranges, so their FRAC_MN values was relatively high.

Metric Changes at the Landscape Level

The landscape pattern metrics of the Changshagongma Wetland Nature Reserve at the landscape level in the four time periods were calculated (**Figure 5**). ED and PD can comprehensively reflect the level of fragmentation in a landscape. The greater the ED and PD values are, the higher the level of landscape fragmentation, and vice versa. From 1992 to 2020, the trends in ED and PD in the study area were similar. ED and PD gradually increased from 1992 to 2013 and reached their highest values (ED, 49.23; PD, 4.03) in 2013. From 2013 to 2020, ED and PD decreased to minimum values of 45.04 and 2.76, respectively. Fragmentation in the study area first increased and then declined. The trend in landscape fragmentation was consistent with that of the sandy grasslands area.

CONTAG reflects the degree of aggregation or disaggregation of different patch classes in a landscape. The higher the CONTAG

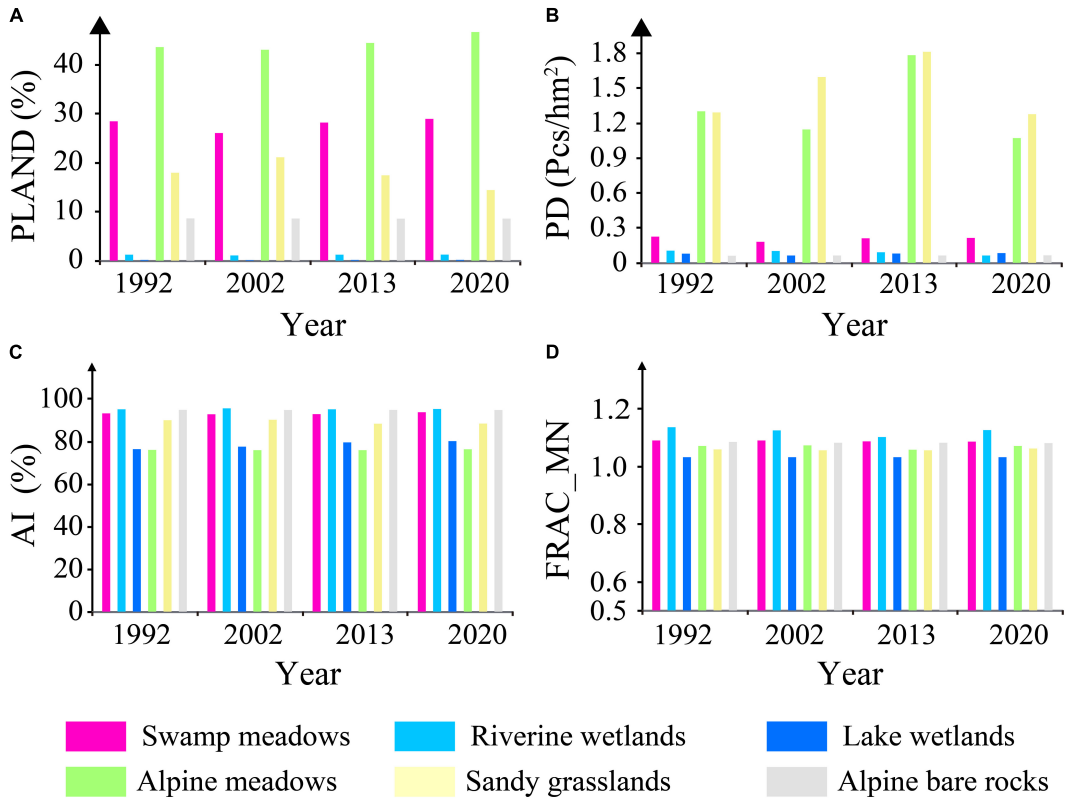

FIGURE 4 | Landscape pattern metrics of the Changshagongma Wetland Nature Reserve at the class level during the four time periods. **(A)** Percentage of landscape (PLAND), **(B)** patch density (PD), **(C)** aggregation index (AI), and **(D)** mean fractal dimension (FRAC_MN).

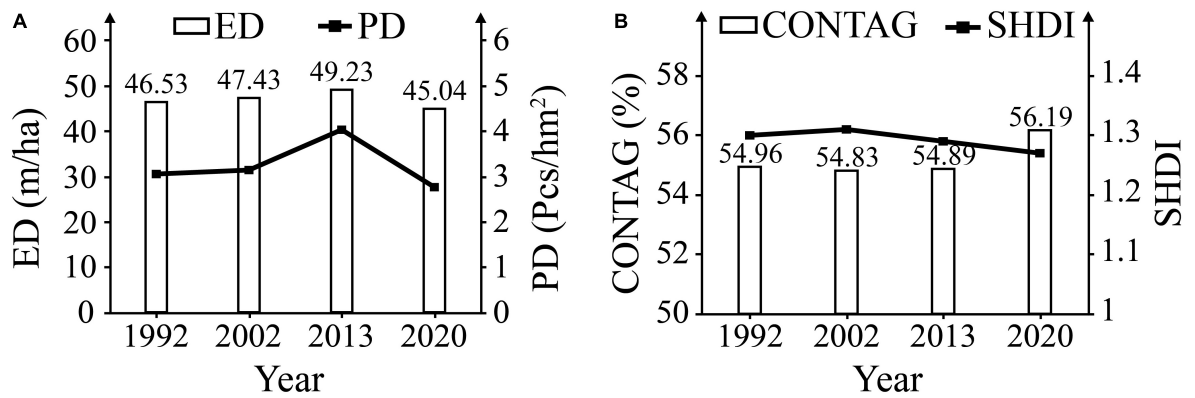

FIGURE 5 | Changes in landscape pattern metrics at the landscape level during the four periods at the Changshagongma Wetland Nature Reserve. **(A)** edge density (ED) and patch density (PD), **(B)** contagion index (CONTAG) and Shannon diversity index (SHDI).

value is, the stronger the connectivity in the landscape, and vice versa. From 1992 to 2020, CONTAG first decreased from 54.96 in 1992 to a lowest value of 54.83 in 2002 and then increased to 54.89 in 2013. It finally increased to a highest value of 56.19 in 2020, indicating that the landscape connectivity in the study area underwent a process of first decreasing and then increasing. The trend in landscape connectivity was consistent with that of the areas of swamp meadows and alpine meadows.

SHDI can reflect the uniformity and heterogeneity of a landscape. The lower the SHDI value is, the more similar the patches and the lower the heterogeneity of the landscape, and vice versa. From 1992 to 2020, the SHDI first increased from 1.30 in 1992 to a highest value of 1.31 in 2002, then decreased to 1.29 in 2013 and finally decreased to a lowest value of 1.26 in 2020. The trend in the SHDI was opposite to that of CONTAG, indicating that the landscape structure of the

study area first became more complicated, and the landscape heterogeneity increased from 1992 to 2002. From 2002 to 2020, the landscape structure tended to be homogeneous, and the landscape distribution tended to be uniform. In 2002, landscape connectivity was the lowest, and landscape heterogeneity was the highest. In 2020, landscape connectivity was the highest, and landscape heterogeneity was the lowest.

Forces Driving the Landscape Pattern

Using bivariate correlations, this paper analyzes the correlations between the landscape pattern index and the eight selected driving factors ($X_1 \sim X_8$) at the type level and the landscape level.

The analysis results at the type level (**Table 5**) show that the bivariate correlation between the landscape pattern index of the dominant landscape (swamp meadows, alpine meadows, and sandy grasslands) and each driving factor is significantly higher than that of other landscapes. The bivariate correlation has the highest significance between the landscape index of the alpine meadows and each driving factor, and it has the lowest significance between the landscape index of the lake wetlands and each driving factor. The correlation between human disturbance (X_8) and the AI of lake wetlands, FRAC_MN of lake wetlands, and PLAND of alpine bare rocks was not significant, and the correlation between human disturbance (X_8) and other landscape pattern indices was significant. In terms of correlation coefficients, most types of landscape pattern indices have lower correlation coefficients with human disturbance than with natural factors, except for swamp meadows. The results showed that natural factors are the main factors affecting the landscape pattern of the Changshagongma Wetland Nature Reserve. The impact of human disturbance on the landscape pattern of the Changshagongma Wetland Nature Reserve cannot be ignored, especially the impact of human disturbance on swamp meadows.

The analysis results at the landscape level (**Table 6**) show that the bivariate correlation between PD, ED, and each driving factor has the strongest significance, followed by SHDI, and CONTAG is the weakest, and the correlation coefficient of PD is larger than that of ED. The correlation between SHDI, CONTAG, and X_6 is not significant, indicating that SHDI, CONTAG, and precipitation have no significant correlation. The correlation between CONTAG and X_1 and X_8 is also not significant, indicating that CONTAG has no obvious correlation with slope aspect and human activities.

Landscape Ecological Risk Analysis

Spatiotemporal Changes in Ecological Risk

The ecological risk of each evaluation cell in the study area was calculated using the landscape ecological risk model. Using the natural breaks method, the ecological risk was divided into five levels: lowest-level risk (I), lower-level risk (II), moderate-level risk (III), higher-level risk (IV), and highest-level risk (V). The spatial distribution is shown in **Figure 6**, and the time series trend is shown in **Figure 7**. In terms of spatial distribution, significant spatial differences were found in ecological risk. The highest-level risk areas were mainly concentrated in the central and southern portions of the Changshagongma Wetland Nature Reserve. The remote sensing classification results also showed that the area of sandy grasslands in these regions was large, indicating that grassland desertification was one of the main threats in terms of ecological risk. The areas with higher-level and moderate-level risk were adjacent to the highest-level risk regions. A small area of moderate-level risk was found in the Zhaqu River basin in the northeast, at the border of Sichuan and Qinghai. Lowest-level risk region were concentrated in the contiguous swamp meadows in the northwest and alpine mountains in the southwest. These regions are largely uninhabited by humans and undergo very little disturbance from human activities. The changes in the average ecological risk in the periods studied followed a hump-shaped trend. The ecological risk increased from 1992 to 2002 and declined continuously from 2002 to 2020. Since 1992, the ecological risk has decreased, and the ecological risk trend has been similar to the trend in climate.

Factors Driving Ecological Risk

Using the Geodetector model, q value changes in factors driving ecological risks in the Changshagongma Wetland Nature Reserve from 1992 to 2020 were detected (**Table 7**). Although the driving factors differed between time periods, the overall driving force of climate characteristics was the highest, followed by topography and geomorphology, and human disturbance had the lowest effect. In 2020, for example, the importance of all indicators was ranked from high to low as $X_5 > X_7 > X_2 > X_8 > X_6 > X_1 > X_3 > X_4$. The influence of the topographic and geomorphological indicators was ranked as $X_2 > X_1 > X_3 > X_4$. From the perspective of changes in the q values of the topographic and geomorphological indicators over time, the changes in X_1, X_3, and X_4 were small. X_2 exhibited relatively large changes, and its q value reached its highest value in 2002, when the ecological risk was the highest, indicating that topography and geomorphology were the greatest drivers. The driving power of aspect, slope, and relief amplitude was low, and its changes were small. The influence of climatic characteristics was ranked from high to low as $X_5 > X_7 > X_6$. Regarding the changes in the q value of the climatic index over time, the q value of X_6 was lowest in 2002. However, the q values of X_5 and X_7 showed the opposite trend, and the q values of X_6 and X_7 were the greatest. These results showed that the q value of X_6 decreased when the climate was cold and dry and increased when it was warm and wet. The driving power of X_8 was greatest in 2002 and then decreased later, indicating that the effect of human activities on the ecological risk of the study area was decreasing.

DISCUSSION

Many alpine wetlands are distributed on the Qinghai-Tibet Plateau. The Changshagongma Wetland Nature Reserve is adjacent to the Three Rivers Source of the Qinghai-Tibet Plateau and is a typical representative of alpine wetlands. Alpine wetlands play an important role in water conservation, climate regulation, carbon and nitrogen deposition, water purification, and biodiversity maintenance (Zhang et al., 2011; Chen et al., 2014). However, studies have shown that the alpine wetland ecosystem of the Qinghai-Tibet Plateau has become an area

TABLE 5 | Bivariate correlations between landscape pattern indices (LPI) and driving factors at the class level.

Minor type	LPI	Topography and geomorphology				Climatic characteristics			Human disturbance
		X_1	X_2	X_3	X_4	X_5	X_6	X_7	X_8
1	PLAND	–0.001	0.236**	–0.364**	–0.485**	–0.359**	–0.164**	–0.373**	0.538**
	PD	–0.099**	–0.014	–0.205**	–0.239**	–0.086**	–0.105**	–0.094**	0.118**
	AI	–0.005	0.190**	–0.203**	–0.290**	–0.245**	–0.082**	–0.247**	0.338**
	FRAC_NN	0.035	–0.011	0.106**	0.109**	0.017	0.109**	0.016	–0.147**
2	PLAND	0.008	–0.471**	–0.222**	–0.031	0.369**	–0.050	0.381**	–0.203**
	PD	0.003	0.026	–0.189**	–0.212**	–0.115**	–0.238**	–0.130**	0.264**
	AI	–0.055	–0.138**	–0.008	0.043	0.165**	0.116**	0.174**	–0.191**
	FRAC_NN	–0.009	–0.296**	–0.027	0.094**	0.254**	0.105**	0.266**	–0.263**
3	PLAND	0.206**	0.087*	–0.049	–0.063	–0.093*	0.112**	–0.110*	0.153**
	PD	0.166**	0.086*	–0.114**	–0.114**	–0.103*	0.071	–0.112**	0.152**
	AI	–0.076	–0.022	0.094*	0.060	0.026	0.001	0.033	–0.068
	FRAC_NN	0.131**	–0.042	0.052	0.034	0.060	0.043	0.023	–0.047
4	PLAND	–0.016	–0.538**	0.304**	0.421**	0.573**	0.127**	0.590**	–0.455**
	PD	–0.060**	0.104**	–0.206**	–0.267**	–0.150**	–0.190**	–0.174**	0.072**
	AI	0.006	–0.276**	0.201**	0.270**	0.306**	0.158**	0.325**	–0.209**
	FRAC_NN	0.141**	0.058**	0.155**	0.198**	0.007	0.100**	0.007	–0.214**
5	PLAND	0.106**	–0.090**	0.125**	0.089**	0.120**	–0.079**	0.080**	–0.256**
	PD	–0.012	0.103**	0.012	0.029	–0.051**	–0.076**	–0.045*	–0.062**
	AI	0.107**	–0.088**	0.001	–0.006	0.068**	–0.108**	0.019	–0.062**
	FRAC_NN	0.182**	–0.100**	0.090**	0.093**	0.131**	0.165**	0.112**	–0.145**
6	PLAND	0.049	0.426**	–0.075*	–0.110**	–0.303**	0.162**	–0.293**	0.036
	PD	0.044	0.093**	–0.041	–0.037	–0.075*	0.070*	–0.058	–0.114**
	AI	–0.020	0.306**	–0.097**	–0.143**	–0.244**	0.056	–0.227**	0.200**
	FRAC_NN	0.009	0.055	–0.075*	–0.069*	–0.078*	–0.079*	–0.087**	–0.064*

1, swamp meadows; 2, riverine wetlands; 3, lake wetlands; 4, alpine meadows; 5, sandy grasslands; and 6, alpine bare rocks.
"" and "**" indicate significant correlations at levels of 0.05 and 0.01, respectively.*

TABLE 6 | Bivariate correlations between landscape pattern indices (LPI) and driving factors at the landscape level.

LPI	Topography and geomorphology				Climatic characteristics			Human disturbance
	X_1	X_2	X_3	X_4	X_5	X_6	X_7	X_8
PD	–0.065**	0.164**	–0.154**	–0.165**	–0.171**	–0.174**	–0.177**	0.036*
ED	0.041*	0.054**	–0.123**	–0.118**	–0.078**	–0.102**	–0.103**	–0.124**
CONTAG	–0.032	–0.248**	0.095**	0.149**	0.244**	0.002	0.260**	0.021
SHDI	–0.057**	0.415**	–0.192**	–0.197**	–0.419**	–0.009	–0.413**	0.133**

"" and "**" indicate significant correlations at levels of 0.05 and 0.01, respectively.*

of rapid change in the landscape pattern of the Qinghai-Tibet Plateau and a high-risk area for ecological security because of its strong sensitivity to climate change (Pan et al., 2007).

Previous attribution studies of the landscape pattern of alpine wetlands have shown that climate change is the dominant factor (Zhao et al., 2012; Du et al., 2015). This understanding is verified in a case study based on the Changshagongma Wetland Nature Reserve (**Tables 6**, **7**), where we found that the explanatory power of temperature is higher than that of precipitation. In empirical understanding, precipitation (including rainfall and snowfall) is the main source of water supply for wetlands, but the amount of precipitation in alpine regions (the proportion of snowfall is higher than that of rainfall) is smaller, and the water in alpine wetlands is not directly replenished by precipitation but more due to warming, which promotes the melting of ice, snow, and seasonally frozen soil, and then the water is supplied to the alpine wetland through the surface (underground) through the snow melting process. Compared to wetlands in low plains (Yang et al., 2021), the hydrological processes of alpine wetlands are more complex and are simultaneously affected by multiple factors, such as topography, alpine ice and snow, frozen soil, air temperature, vegetation, and human activities. The amount of water produced by melting ice, snow, and permafrost is regulated by changes in air temperature, which makes the effect of temperature in the change process of alpine wetlands more obvious and direct. Under global climate change, the temperature of the Qinghai-Tibet Plateau has increased significantly, and its climate is trending toward warming and humidification (Xu et al., 2019).

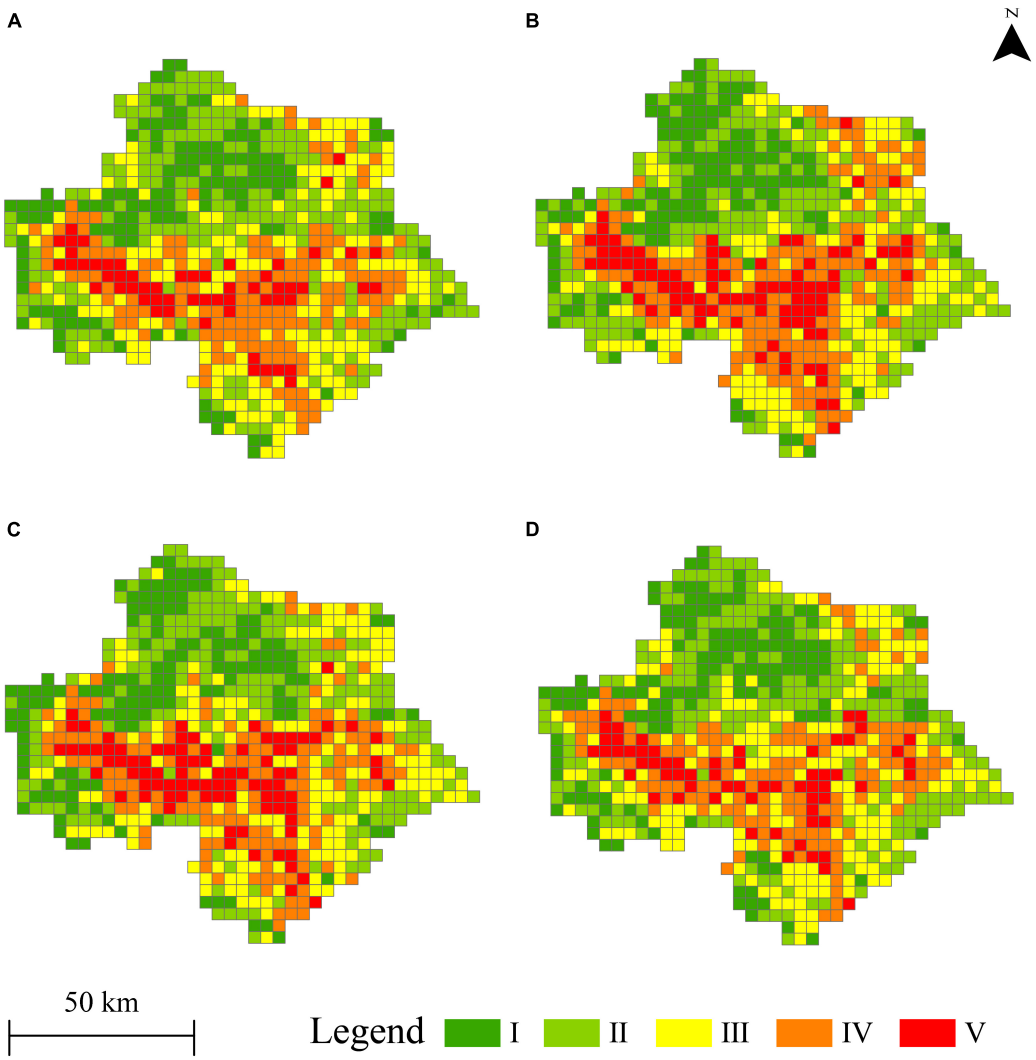

FIGURE 6 | Temporal and spatial distribution of ecological risk during the four periods in the Changshagongma Wetland Nature Reserve. **(A)** 1992, **(B)** 2002, **(C)** 2013, **(D)** 2020.

The warming of the Qinghai-Tibet Plateau has accelerated the melting of ice and snow, which has increased the water supply of wetlands to varying degrees, resulting in a rise of the water level and an increase in the area of wetlands such as lakes and swamps, and the meadows tend to become swampy (Mao et al., 2021). At the same time, continuous warming increases the amount of permafrost ablation, which leads to surface water infiltration or recharge of underground runoff, which directly affects the groundwater recharge in alpine wetlands and changes wetland water storage, resulting in fluctuations in wetland area (Jin et al., 2009; Liu and Wang, 2012). The Qinghai-Tibet Plateau is increasingly affected by global changes coupled with the vulnerability of alpine wetlands and their sensitivity to climate change. The future warming scenario may cause the wetland landscape pattern to show significant volatility, which will have various impacts on the ecological security of alpine wetlands (Xu et al., 2019; Jin et al., 2020). Therefore, in future research on alpine wetlands, attention should be paid to the impact of local hydrological processes on the landscape of alpine wetlands, revealing the changing laws of alpine wetlands from hydrological processes and then proposing corresponding measures for the conservation and restoration of alpine wetlands in changing environments.

In existing studies, scholars have actively explored the degree of interference of human activities on various wetlands on the Qinghai-Tibet Plateau and found that it was generally weak but varied in different regions (Zhao et al., 2015; Liu et al., 2019). The case of Zoige has shown that human disturbance has significantly affected the changes and ecological security of wetland landscape patterns (Li et al., 2014). Most of the wetlands on the Qinghai-Tibet Plateau are located in nature reserves, with very few human activities, and spatial data to quantitatively describe them are lacking. Because of this limitation, most of the existing studies have carried out qualitative analysis, and accurately assessing the

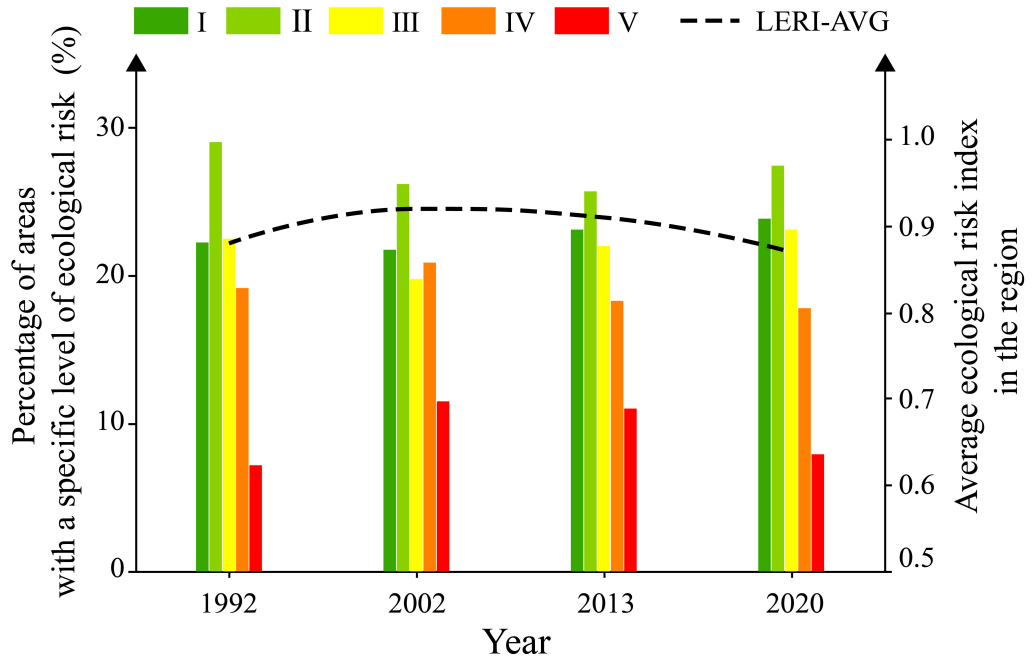

FIGURE 7 | Time series trend in ecological risk during the four periods at the Changshagongma Wetland Nature Reserve.

TABLE 7 | *q* values of driving factors from 1992 to 2020 (%).

	Topography and geomorphology				Climatic characteristics			Human disturbance
	X_1	X_2	X_3	X_4	X_5	X_6	X_7	X_8
1992	10.34	23.67	5.46	4.39	28.75	9.68	25.45	21.51
2002	10.24	27.99	4.68	4.63	34.77	7.06	31.96	24.87
2013	13.21	19.37	5.36	5.28	26.31	17.22	21.44	19.80
2020	11.23	20.80	5.24	4.00	29.22	11.03	25.33	18.23

impact process and intensity of human disturbance on different alpine wetlands is difficult (Qiu et al., 2009). In this case, we try to take the distance between the landscape unit and the road as the interference degree of human activities on wetland ecological security in the Changshagongma Wetland Nature Reserve to reveal the interference process of human footprints on alpine wetlands to a certain extent. The results showed that, overall, human activities have a weak disturbance on wetland landscapes. However, the analysis results at the type level of the landscape pattern index found that human disturbance had a significant impact on the landscape pattern changes in swamp meadows (**Table 5**). Swamp meadows are transitional wetlands between meadows and swamps, and changes in their landscape patterns are related to wetland succession and development. The strong disturbance of swamp meadows by human activities showed that swamp meadows, as fragile and sensitive areas in wetland conservation, are extremely vulnerable to human activities and present ecological security risks. This attribute warns wetland protectors and managers to continue to carry out engineering measures such as returning grazing land to grassland and wetland restoration in the future. At the same time, "the most beautiful wetland" is the business card of Shiqu County's tourism development. In recent years, the number of tourists has gradually increased, which will surely make the Changshagongma Wetland Nature Reserve bear the pressure of tourism development. Wetland protectors and managers should scientifically guide the development of tourism, strengthen ecological protection publicity for tourists, and avoid disorderly tourism and reckless driving.

CONCLUSION

We completed the fourth phase (1992, 2002, 2013, 2020) of wetland classification of the Changshagongma Wetland Nature Reserve using the GEE platform, analyzed the climate change trends, revealed the evolution characteristics of wetland landscape patterns, and assessed ecological risk and the explanatory power of driving factors. The main conclusions are as follows:

(1) The main land cover (LULC) types in the Changshagongma Wetland Nature Reserve were swamp

meadows, alpine meadows, and sandy grasslands. Swamp meadows were the main type of wetland, and the distribution was relatively concentrated. From 1992 to 2020, the overall area of wetlands showed a "∨"-shaped change trend.

(2) Throughout the analysis period (1992–2020), the wetland landscape pattern of the Changshagongma Wetland Nature Reserve was optimized, which was reflected in the enhancement of spatial connectivity and the reduction of fragmentation and heterogeneity. However, differences are observed between periods. In the early period (1992–2002), the climate was cold and dry, and coupled with high-intensity grazing, the wetland area decreased, and the sandy grassland expanded, resulting in an increase in landscape fragmentation and heterogeneity. In the later period (2002–2020), the climate was warm and humid, and projects such as returning grazing land to grassland and wetland restoration were implemented in the region. The wetland area increased, the sandy grassland area decreased, the landscape fragmentation was reduced, and the spatial connectivity was enhanced.

(3) The results of the ecological risk assessment showed obvious spatial heterogeneity in the ecological risk of the Changshagongma Wetland Nature Reserve (**Figure 6**). The results showed that the topographic difference and the interference intensity of human activities were the main reasons for the internal spatial differentiation of landscape ecological risk.

(4) Overall, climate change had the greatest impact on the ecological risk of wetland landscapes in the Changshagongma Wetland Nature Reserve, followed by topographical conditions and lesser human activities. Among them, because of the special hydrological process of alpine wetlands, air temperature and evapotranspiration had a greater impact on the wetland landscape. Although the overall impact of human activities on the landscape pattern was weak, the explanatory power of the landscape pattern index at the type level found that swamp meadows were strongly disturbed by human activities and became fragile and sensitive zones that should be focused on in wetland conservation and management.

The landscape ecological risk model constructed based on the landscape pattern index in this paper can better evaluate and identify the main controlling factors of ecological risk in alpine and humid regions. However, the scale effects in the data, classification criteria, and models may affect the results and therefore cannot be ignored. The Changshagongma Wetland Nature Reserve and other alpine wetland areas have many small wetlands (small wetlands play an important role in maintaining biodiversity, regulating water sources, etc.), but limited by medium-resolution image data, the interpretation of small wetlands is not precise and comprehensive enough, and the complex succession process of wetland landscapes is easily ignored at fine scales. In further research, high-resolution image data can be used to strengthen the fine observation of small and micro wetlands. While improving the data accuracy, the subjectivity in the wetland classification system should also be considered. Different landscape classification systems have different impacts on the calculation of landscape patterns, which may damage the credibility and universality of the research results. Follow-up research should focus on the characteristics of alpine wetlands to establish a common wetland identification and classification standard to improve the contrast of case studies. In the model, the grid-based landscape index calculation has a plastic area unit problem; that is, the index is sensitive to the setting of the landscape unit scale, and the calculation results may depend on scale grid units, so future research should pay more attention to the scale effect of landscape ecological risk.

DATA AVAILABILITY STATEMENT

The original contributions presented in the study are included in the article/supplementary material, further inquiries can be directed to the corresponding author.

AUTHOR CONTRIBUTIONS

CY and WD contributed to the writing of the manuscript and concept of the study. CY, SZ, and QY were involved in the field work and data collection. CY, WD, QY, and SZ provided important guidance on methods and writing. All authors contributed critically to drafts and gave approval for publication.

FUNDING

This research was supported by a key project of the National Natural Science Foundation of China (Grant No. 41930651).

ACKNOWLEDGMENTS

We would like to thank the Shiqu County Government of Sichuan Province for its assistance in the field investigation, Zhu Dan for his suggestions for our study, and Zhang Hao and Chen Liang-shuai for their helpful discussions.

REFERENCES

Bai, J. H., Lu, Q. Q., Wang, J. J., Zhao, Q. Q., Ouyang, H., Deng, W., et al. (2013). Landscape pattern evolution processes of alpine wetlands and their driving factors in the Zoige Plateau of China. *J. Mount. Sci.* 10, 54–67. doi: 10.1007/s11629-013-2572-1

Chen, H., Yang, G., Peng, C. H., Zhang, Y., Zhu, D., Zhu, Q. A., et al. (2014). The carbon stock of alpine peatlands on the Qinghai-Tibetan Plateau during the Holocene and their future fate. *Quat. Sci. Rev.* 95, 151–158. doi: 10.1016/j.quascirev.2014.05.003

Chen, K. M., and Zhu, X. D. (2021). Remote Sensing of Spatio-temporal Dynamics of Saltmarsh Vegetation along South China

Coast based on Google Earth Engine. *Remote Sensing Nat. Res.* 36, 751–759.

Chen, T. Q., Feng, Z., Zhao, H. F., and Wu, K. N. (2020). Identification of ecosystem service bundles and driving factors in Beijing and its surrounding areas. *Sci. Total Environ.* 711:134687. doi: 10.1016/j.scitotenv.2019.134687

Cong, P. F., Chen, K. X., Qu, L. M., and Han, J. B. (2019). Dynamic Changes in the Wetland Landscape Pattern of the Yellow River Delta from 1976 to 2016 Based on Satellite Data. *Chin. Geograph. Sci.* 29, 372–381. doi: 10.1007/s11769-019-1039-x

Cui, G., Liu, Y., and Tong, S. Z. (2021). Analysis of the causes of wetland landscape patterns and hydrological connectivity changes in Momoge National Nature Reserve based on the Google Earth Engine Platform. *Arabian J. Geosci.* 14:16. doi: 10.1007/s12517-021-06568-8

Du, J., Wang, G., Yang, Y., Zhang, T., and Tianxu, M. (2015). Temporal and spatial variation of the distributive patterns and driving force analysis in the Yangtze River and Yellow River source regions wetland. *Acta Ecol. Sin.* 35, 6173–6182.

Du, Z. Q., Zhang, X. Y., Xu, X. M., Zhang, H., Wu, Z. T., and Pang, J. (2017). Quantifying influences of physiographic factors on temperate dryland vegetation, Northwest China. *Sci. Rep.* 7:40092. doi: 10.1038/srep40092

Hou, M. J., Ge, J., Gao, J. L., Meng, B. P., Li, Y. C., Yin, J. P., et al. (2020). Ecological Risk Assessment and Impact Factor Analysis of Alpine Wetland Ecosystem Based on LUCC and Boosted Regression Tree on the Zoige Plateau. *China. Remote Sens.* 12:368. doi: 10.3390/rs12030368

Huang, C., Chen, Y., Zhang, S. Q., and Wu, J. P. (2018). Detecting, Extracting, and Monitoring Surface Water From Space Using Optical Sensors: A Review. *Rev. Geophys.* 56, 333–360. doi: 10.1029/2018rg000598

Inkoom, J. N., Frank, S., Greve, K., Walz, U., and Furst, C. (2018). Suitability of different landscape metrics for the assessments of patchy landscapes in West Africa. *Ecol. Indicat.* 85, 117–127. doi: 10.1016/j.ecolind.2017.10.031

Jin, H. J., He, R. X., Cheng, G. D., Wu, Q. B., Wang, S. L., Lu, L. Z., et al. (2009). Changes in frozen ground in the Source Area of the Yellow River on the Qinghai-Tibet Plateau, China, and their eco-environmental impacts. *Environ. Res. Lett.* 4:045206. doi: 10.1088/1748-9326/4/4/045206

Jin, X., Jin, Y. X., and Mao, X. F. (2019). Ecological risk assessment of cities on the Tibetan Plateau based on land use/land cover changes - Case study of Delingha City. *Ecol. Indicat.* 101, 185–191. doi: 10.1016/j.ecolind.2018.12.050

Jin, Z., You, Q. L., Wu, F. Y., Sun, B., and Cai, Z. Y. (2020). Changes of climate and climate extremes in the Three-Rivers Headwaters' Region over the Tibetan Plateau during the past 60 years. *Transact. Atmos. Sci.* 43, 1042–1055.

Kumar, L., and Mutanga, O. (2018). Google Earth Engine Applications Since Inception: Usage, Trends, and Potential. *Remote Sens.* 10:15. doi: 10.3390/rs10101509

Li, H. B., and Wu, J. G. (2004). Use and misuse of landscape indices. *Landscape Ecol.* 19, 389–399. doi: 10.1023/B:LAND.0000030441.15628.d6

Li, Z. W., Wang, Z. Y., Zhang, C. D., Han, L. J., and Zhao, N. (2014). A study on the mechanism of wetland degradation in Ruoergai swamp. *Adv. Water Sci.* 25, 172–180.

Liu, G. L., Zhang, L. C., Zhang, Q., Musyimi, Z., and Jiang, Q. H. (2014). Spatio-Temporal Dynamics of Wetland Landscape Patterns Based on Remote Sensing in Yellow River Delta, China. *Wetlands* 34, 787–801. doi: 10.1007/s13157-014-0542-1

Liu, G. S., and Wang, G. X. (2012). Insight into runoff decline due to climate change in China's Water Tower. *Water Sci. Technol. Water Supply* 12, 352–361. doi: 10.2166/ws.2012.003

Liu, S. L., Cui, B. S., Dong, S. K., Yang, Z. F., Yang, M., and Holt, K. (2008). Evaluating the influence of road networks on landscape and regional ecological risk-A case study in Lancang River Valley of Southwest China. *Ecol. Engineer.* 34, 91–99. doi: 10.1016/j.ecoleng.2008.07.006

Liu, Z., Li, S., Wel, W., and Song, X. (2019). Research progress on alpine wetland changes and driving forces in Qinghai-Tibet Plateau during the last three decades. *Chin. J. Ecol.* 38, 856–862. doi: 10.13292/j.1000-4890.201903.002

Ma, L. B., Bo, J., Li, X. Y., Fang, F., and Cheng, W. J. (2019). Identifying key landscape pattern indices influencing the ecological security of inland river basin: The middle and lower reaches of Shule River Basin as an example. *Sci. Total Environ.* 674, 424–438. doi: 10.1016/j.scitotenv.2019.04.107

Mahdavi, S., Salehi, B., Granger, J., Amani, M., Brisco, B., and Huang, W. M. (2018). Remote sensing for wetland classification: a comprehensive review. *Gisci. Remote Sens.* 55, 623–658. doi: 10.1080/15481603.2017.1419602

Mao, D., Wang, Z., Wang, Y., Choi, C. Y., Jia, M., Jackson, M. V., et al. (2021). Remote Observations in China's Ramsar Sites: Wetland Dynamics, Anthropogenic Threats, and Implications for Sustainable Development Goals. *J. Remote Sens.* 2021, 1–13. doi: 10.34133/2021/9849343

Pan, J. H., Wang, J., and Wang, J. H. (2007). Dynamic Change of Frigid Wetlands in Source Region of the Yangtze and Yellow Rivers. *Wetland Sci.* 5, 298–304.

Pei, H., Wei, Y., Wang, X., Qin, Z. H., and Hou, C. L. (2014). Method of cultivated land landscape ecological security evaluation and its application. *Transact. Chin. Soc. Agricult. Engin.* 30, 212–219.

Qiu, P. F., Wu, N., Luo, P., Wang, Z. Y., and Li, M. H. (2009). Analysis of dynamics and driving factors of wetland landscape in Zoige, Eastern Qinghai-Tibetan Plateau. *J. Mountain Sci.* 6, 42–55. doi: 10.1007/s11629-009-0230-4

Santos, X., Brito, J. C., Sillero, N., Pleguezuelos, J. M., Llorente, G. A., Fahd, S., et al. (2006). Inferring habitat-suitability areas with ecological modelling techniques and GIS: A contribution to assess the conservation status of Vipera latastei. *Biol. Conser.* 130, 416–425. doi: 10.1016/j.biocon.2006.01.003

Shen, G., Yang, X. C., Jin, Y. X., Xu, B., and Zhou, Q. B. (2019). Remote sensing and evaluation of the wetland ecological degradation process of the Zoige Plateau Wetland in China. *Ecol. Indicat.* 104, 48–58. doi: 10.1016/j.ecolind.2019.04.063

Shi, H., Yang, Z. P., Han, F., Shi, T. G., and Li, D. (2015). Assessing Landscape Ecological Risk for a World Natural Heritage Site: a Case Study of Bayanbulak in China. *Polish J. Environ. Stud.* 24, 269–283. doi: 10.15244/pjoes/28685

Wang, H., Gao, J. B., and Hou, W. J. (2019). Quantitative attribution analysis of soil erosion in different geomorphological types in karst areas: Based on the geodetector method. *J. Geograph. Sci.* 29, 271–286. doi: 10.1007/s11442-019-1596-z

Wang, J. F., and Xu, C. D. (2017). Geodetector: Principle and prospective. *Acta Geogr. Sin.* 72, 116–134.

Wang, X. X., Xiao, X. M., Zou, Z. H., Hou, L. Y., Qin, Y. W., Dong, J. W., et al. (2020). Mapping coastal wetlands of China using time series Landsat images in 2018 and Google Earth Engine. *ISPRS J. Photogram. Remote Sens.* 163, 312–326. doi: 10.1016/j.isprsjprs.2020.03.014

Wang, Z., Xu, W. G., Xia, X., Yu, H. X., Lv, Y. Y., and Zhang, J. L. (2021). Novel Quantitative Method for Assessing Driving Forces of Landscape Succession: Case Study From Yancheng Coast, China. *Front. Ecol. Evol.* 9:632331. doi: 10.3389/fevo.2021.632331

Wu, J. G. (2004). Effects of changing scale on landscape pattern analysis: scaling relations. *Landscape Ecol.* 19, 125–138. doi: 10.1023/B:LAND.0000021711.40074.ae

Xu, L. J., Hu, Z. Y., Zhao, Y. N., and Hong, X. Y. (2019). Climate Change Characteristics in Qinghai-Tibetan Plateau during 1961-2010. *Plateau Meteorol.* 38, 911–919.

Yang, M., Gong, J. G., Zhao, Y., Wang, H., Zhao, C. P., Yang, Q., et al. (2021). Landscape Pattern Evolution Processes of Wetlands and Their Driving Factors in the Xiong'an New Area of China. *Int. J. Environ. Res. Public Health* 18:4403. doi: 10.3390/ijerph18094403

Yao, J. P., Yang, L. K. C. T., and Song, C. Q. (2021). Consecutive monitoring of the poyang lake wetland by integrating sentinel-2 with sentinel-1 and landsat 8 data. *Remote Sensing Nat. Res.* 36, 760–776.

Yuan, L. H., Chen, X. Q., Wang, X. Y., Xiong, Z., and Song, C. Q. (2019). Spatial associations between NDVI and environmental factors in the Heihe River Basin. *J. Geograph. Sci.* 29, 1548–1564. doi: 10.1007/s11442-019-1676-0

Yue, Q. F., Zhao, X. Q., Li, S., Tan, K., Pu, J. W., and Wang, Q. (2021). Landscape pattern changes and ecological risk in the Padam River Basin under the background of the "Belt and Road" lnitiative. *World Region. Stud.* 30, 839–850.

Zhang, Y., Wang, G. X., and Wang, Y. B. (2011). Changes in alpine wetland ecosystems of the Qinghai-Tibetan plateau from 1967 to 2004. *Environ. Monit. Assess.* 180, 189–199. doi: 10.1007/s10661-010-1781-0

Zhao, F., Liu, H., Zhang, H., and Zou, W. (2012). Driving Forces for Wetland Changes in the Typical Region of the Origin of the Three Major Rivers. *Wetland Sci. Manage.* 8, 57–60.

Zhao, Z. L., Zhang, Y. L., Liu, L. S., Liu, F. G., and Zhang, H. F. (2015). Recent changes in wetlands on the Tibetan Plateau: A review. *J. Geograph. Sci.* 25, 879–896. doi: 10.1007/s11442-015-1208-5

Zhu, L. J., Meng, J. J., and Zhu, L. K. (2020). Applying Geodetector to disentangle the contributions of natural and anthropogenic factors to NDVI variations in the middle reaches of the Heihe River Basin. *Ecol. Indicat.* 117:106545. doi: 10.1016/j.ecolind.2020.106545

Conflict of Interest: The authors declare that the research was conducted in the absence of any commercial or financial relationships that could be construed as a potential conflict of interest.

Publisher's Note: All claims expressed in this article are solely those of the authors and do not necessarily represent those of their affiliated organizations, or those of the publisher, the editors and the reviewers. Any product that may be evaluated in this article, or claim that may be made by its manufacturer, is not guaranteed or endorsed by the publisher.